Taylor & Francis
Taylor & Francis Group

ORIGINAL RESEARCH

🔓 OPEN ACCESS | Check for updates

PD-L1 blockade potentiates the antitumor effects of ALA-PDT and optimizes the tumor microenvironment in cutaneous squamous cell carcinoma

Qingyu Zeng [ID][#], Jiayi Yang [ID][#], Jie Ji, Peiru Wang, Linglin Zhang, Guorong Yan [ID], Yuhao Wu, Qi Chen, Jia Liu, Guolong Zhang [ID], and Xiuli Wang [ID]

Institute of Photomedicine, Shanghai Skin Disease Hospital, School of Medicine, Tongji University, Shanghai, China

ABSTRACT

Immune checkpoint blockade (ICB) is a powerful oncologic treatment modality for a wide variety of human malignancies, but the patient response rate to this treatment remains low, especially in patients with cutaneous squamous cell carcinoma (cSCC). 5-Aminoleuvulinic acid-photodynamic therapy (ALA-PDT) is widely used to treat cancerous and precancerous skin diseases, but the value of ALA-PDT in the treatment of invasive cSCC is debatable. Our previous studies have shown that ALA-PDT can induce antitumor immune responses by promoting the immunogenic death of tumor cells. However, it is unclear whether ALA-PDT exerts synergistic effects with ICB in cSCC. Here, we report that PD-L1 blockade potentiates the antitumor effects of ALA-PDT both on primary and distant tumors, and optimizes the tumor microenvironment in cSCC. In this study, we first detected PD-L1 expression in patients with different grades of cSCC. Then we found the combination of anti-PD-L1 monoclonal antibody (mAb) and ALA-PDT killed tumor cells by apoptosis- and/or ferroptosis-mediated immunogenic cell death (ICD) and stimulated systemic immune response, as well as building the immunological memory response to prevent tumor recurrence. Furthermore, we found that combination therapy can be used to recruit tertiary lymphoid structure (TLS)-like intratumoral lymphoid aggregates, which may promote tumor-infiltrating lymphocyte (TIL)-mediated antitumor immunity. In summary, our work demonstrates that ICB treatment with an anti-PD-L1 antibody is a promising strategy that may potentiate the antitumor effects of ALA-PDT in cSCC.

Introduction

cSCC is the second most common malignant tumor of the skin. Although cSCC is characterized by approximately 5% metastasis and is associated long-term survival after treatment,[1,2] the aging and growing population has led to an increasing incidence and mortality rate of cSCC worldwide.

ICB is a powerful oncologic treatment modality for a wide variety of human cancers.[3,4] Blockade of CTLA-4 and PD-1/PD-L1 has achieved impressive clinical responses and revolutionized the treatment of many cancers. However, only a fraction of cSCC patients (not enough 50% objective response) respond to ICB therapies, and most responders suffer tumor recurrence due to tumor cells evading the immune system.[5,6] Thus, the development of new combination treatments is a major focus of current cancer immunotherapy studies.

ALA-PDT is an increasingly important therapeutic modality for the treatment of cancer because it shows spatiotemporal selectivity and minimal side effects, does not induce intrinsic resistance, has a noninvasive nature and shows a favorable safety profile. ALA-PDT involves the delivery of photosensitizers to the tumor site and subsequent irradiation with certain wavelengths of light to generate cytotoxic $^1O_2$ from molecular oxygen. In elderly individuals, cSCC is common in the face and genital area; in areas where tumors are difficult to remove, the benefits of ALA-PDT enable the preservation of organ function and are recommended for the treatment of cSCC in situ according to European guidelines.[7,8]

Although the efficacy and safety of ALA-PDT have been widely studied, the value of using ALA-PDT in the treatment of large skin lesions or invasive cSCC is debatable, and ALA-PDT has consistently failed to achieve the ideal effect due to the heterogeneity and complexity of tumors.[9–13] A challenge in oncology is the rational and effective integration of immunotherapy with traditional treatments, including ALA-PDT. We previously found that immune system activation is an integral part of ALA-PDT-mediated antitumor effects. ALA-PDT promoted DAMPs (CRT, HSP70 and HMGB1) release in the treatment of cSCC mouse model and stimulated the maturation of DCs concomitantly.[14,15] The immunogenic cell death induced by PDT was further confirmed by using photosensitizers such as redaporfin,[16,17] rose Bengal,[18] photosens and photodithazine.[19] These results implied that PDT is an effective approach of inducing ICD. Because of the antitumor immune response it induces, ICB may compensate for the

---

insufficiency of ALA-PDT, and combination therapy with mutually beneficial ICB and ALA-PDT may be a promising strategy for cSCC treatment.

TLSs are ectopic lymphoid organs that develop in nonlymphoid tissues at sites of chronic inflammation, including tumors.[20–22] TLSs are composed of a T cell-enriched zone with mature DCs juxtaposing a B-cell follicle with germinal center characteristics and are surrounded by plasma cells. The described correlation between TLSs and clinical benefit in patients with cancer, suggests that TLSs may be prognostic and predictive factors, and interest into investigating the role of TLSs in tumors has increased.[23,24] Therefore, we were interested in determining whether the adaptive immunity activation through combination therapy is associated with TLS formation.

Here, we first detected PD-L1 expression in patients with different grades of cSCC. Then we investigated the synergistic effects of ALA-PDT and an anti-PD-L1 mAb on primary and distant tumor growth in an implanted cSCC mouse model and a UV-induced cSCC mouse model. We further studied the regulatory effects of ICD caused by combination therapy on tumor-infiltrating lymphocytes and immunological memory response. In addition, we demonstrated that the antitumor immune function of ALA-PDT may be mediated by TLSs in cSCC. Hence, this study support the idea that combination therapy as an immunotherapeutic modality targeting PD-L1 and ALA-PDT may have the potential to attenuate cSCC.

Materials and methods

Ethics statement

The Institutional Research Medical Ethics Committee of Shanghai Skin Disease Hospital approved this study (approval no. 2021–29). Written informed consent was obtained from all patients. All experimental protocols were performed according to the guidelines of the Declaration of Helsinki.

Cell lines

The A431 human epidermoid carcinoma (ATCC) cell line was maintained in DMEM (HyClone) supplemented with 10% FBS (Gibco), 100 U/ml penicillin, and 100 U/ml streptomycin at 37 ℃ in a humidified incubator containing 5% CO_2.

Mouse model construction

Seven-week-old SKH-1 mice were purchased from the Shanghai Laboratory Animal Center. Two mouse models were established in this study: a UV-induced cSCC mouse model and an implanted cSCC mouse model.

Constituting the UV-induced cSCC mouse model, mice in the ultraviolet radiation (UVR) group were irradiated with ultraviolet rays from an SUV1000 daylight ultraviolet simulator (Sigma) with built-in UVA and UVB filters. The initial minimal erythema dose (MED) was 160 mJ/cm^{2} for UVB and 2520 mJ/cm^{2} for UVA.[25,26] UV radiation was administered four times every week for 28 weeks. As the mice showed an increased tolerance to UVR, the light dose was enhanced until 1.625 MED was reached through 20 weeks. At the end of the experiment, the cumulative doses of UVA and UVB were 242.91 J/cm^{2} and 26.99 J/cm^{2}, respectively. The tumor diameters in the UVR group were recorded weekly.

To generate an implanted cSCC mouse model, XL50 cells (mouse cSCC cells; 5×10^6) and NIH/3T3 cells (1×10^6) were injected subcutaneously into the backs of mice to establish an implanted cSCC mouse model. After 14 days, the tumor-bearing mice were used for the study when the tumor volume reached approximately 7 mm in diameter.

ALA-PDT

Mice with cSCC tumors were anesthetized with inhaled isoflurane and received PDT. ALA cream (8%) was applied externally around the tumor at approximately 1-mm thickness for 3 h. Subsequently, the mice were exposed to 633 nm red LED light at a dose of 38.4 J/cm^{2}.

Western blot assay

Western blotting was performed as described previously.[27] Cell membrane proteins were obtained by using the Cell Surface Protein Isolation Kit (Thermo Fisher Scientific). The antibodies against the following proteins were used: SLC7A11, GPX4, COX2, cleaved PARP (Abcam); CRT, ERp57 (Cell Signaling Technology); HSP70 (Affinity); and Na-K-ATPase (Abbkine). Goat anti-rabbit IgG-horseradish peroxidase (HRP) and goat anti-mouse IgG-HRP (Proteintech) were the secondary antibodies.

Detection of cytokines

TNF-α and IFN-γ in serum samples of mice were measured with Elisa kits ((R&D) according to the manufacture's protocol.

qRT–PCR assay

Total tissue RNA was extracted using TRIzol reagent (Thermo Scientific) according to the manufacturer's recommendations. First-strand cDNA synthesis was performed using Prime Script RT Master Mix (TaKaRa). qRT–PCR was performed using a standard SYBR Green PCR kit (Thermo). The relative expression of genes was calculated using the power formula: $2^{-\Delta\Delta Ct}$. qRT–PCR was performed on a Roche LightCycler 480 system. The following primer sequences were used as follows:

Primer	Sequence (5′-3′)
TNF-α	Fwd-GAAAAGACACCATGAGCACA
	Rev-CCCCGAAGTTCAGTAGACAG
IL-12	Fwd- CAATCACGCTACCTCCTCTT
	Rev-TCAGCAGTGCAGGAATAATG
IL-10	Fwd-AGAGACTTGCTCTTGCACTACC
	Rev- GGAAGTGGGTGCAGTTATTG
IL-4	Fwd- CACTGACGGCACAGAGCTAT
	Rev- TGTGACCTCGTTCAAAATGC
IL-13	Fwd- ACAAGACCAGACTCCCCTGT
	Rev- GAGGCCATGCAATATCCTCT
IFN-γ	Fwd- TGCATCAACCAAAGAAGTATTTA
	Rev- GCAATCACAGTCTTGGCTAAT
CCL8	Fwd- TGCTGCTCATAGCTGTCCCT
	Rev- CATGGGGCACTGGATATTGT

Primer	Sequence (5´-3´)
CXCL13	Fwd- GCTCAAGCTCCGTTGCATAC
	Rev- GGTTTTCATTCCTCGACAATC
CCL21a	Fwd- CGAGGCTATAGGAAGCAAGA
	Rev- ACTTAGAGGTTCCCCGGTTC
CCL21b	Fwd- CGGAAGCACTCTAAGCCTGA
	Rev- CTTGAGGGCTGTGTCTGTTC
CCL2	Fwd- TTGTCACCAAGCTCAAGAGA
	Rev- TACGGGTCAACTTCACATTC
CXCL9	Fwd- ACAGTGGAGACCACCAGAGT
	Rev- ACAGCCACAACCTTCTAGGA
CCL19	Fwd- CTGTGGCCTGCCTCAGATTAT
	Rev- CATTAAGAAGGTAGCGGAAGGC

Histologic analysis

For IHC analysis, the tissue was stored in formalin, and 5 μm sections were dewaxed (30 min at 56 ℃ and treated twice with xylene for 10 min each time), followed by rehydration, antigen unmasking, and blocking. Then, the samples were stained with primary antibodies at 1 μg/mL in blocking solution for 30 min at 37 ℃. The slides were rinsed in PBS and incubated with the appropriate secondary antibody diluted in blocking solution for 30 min. The slides were incubated with streptavidin-biotin complex for 30 min, rinsed in PBS, stained using DAB chromogen and hematoxylin counterstain, and observed under a light microscope. The PD-L1 expression grade and cSCC differentiation grade were determined by two pathology doctors, respectively.

Flow cytometry analysis

Tumors were harvested, and single-cell suspensions were generated through enzymatic digestion at 37°C for 1 hour in DMEM containing collagenase (1 mg/mL, Sigma), hyaluronidase (0.1 mg/mL, Sigma) and DNase (200 U/mL, Sigma) or via mechanical dissociation from the collected tissues. Erythrocytes were lysed in red blood cell lysis buffer (Sigma). Cells were washed twice with PBS and stained with antibodies according to the manufacturer's protocols.

Statistical analysis

All quantified data are expressed as the mean values ± standard error (mean ± SE). Student's t test for nonpaired replicates was performed to identify statistically significant differences between treatment means. Group variability and interaction were compared using either one-way or two-way ANOVA followed by Bonferroni's posttest to compare replicate means. Differences were considered significant when $p < 0.05$.

Results

PD-L1 expression is correlated with the progression of cSCC

To explore the relationship between PD-L1 expression level and cSCC progression, we first examined PD-L1 expression in a tumor-related database. As shown in Figure 1a, elevated PD-L1 expression was observed in cSCC tumors compared to that in normal tissues (left panel, data from the gene expression omnibus database with accession number GSE108010; right panel, Riker melanoma data from the Oncomine database). Furthermore, we analyzed PD-L1 expression using IHC (Figure 1b) with 28 cSCC patient samples and found that the PD-L1 expression score was higher in poorly differentiated tumor tissues than in well-differentiated tumor tissues (Figure 1c).

Chronic sun exposure is the most important and well-known environmental factor associated with cSCC.[28,29] We established a UV-induced cSCC mouse model to imitate human cSCC. As shown in Figure 1e, after exposure to UV for 20 weeks, the skin of the mice showed photoaging, actinic keratosis (AK, pre-cSCC), and, eventually, cSCC. In addition, we found that PD-L1 expression was extremely positive in tumor tissues of the UV-induced cSCC mouse model (Figure 1d). This ensured that the mouse model we used effectively approximated the pathological state of human cSCC. Collectively, these results indicated that PD-L1 expression is correlated with the progression of cSCC.

Synergistic antitumor effects of an anti-PD-L1 mAb and ALA-PDT in an implanted cSCC mouse model

We next investigated whether an anti-PD-L1 mAb and ALA-PDT have synergistic antitumor effects *in vivo*. A bilateral mouse tumor model was developed by subcutaneously injecting XL50 mouse cSCC cells into both the left and right flank regions of SKH-1 mice. The right tumors were designated primary tumors and subjected to local light irradiation, and the left tumors were designated distant tumors and not treated with ALA-PDT. Mice were randomly divided into four groups and received treatment as shown in Figure 2a. Measurements of tumor volume showed that the combination treatment with an anti-PD-L1 mAb and ALA-PDT significantly decreased the growth of primary tumors and distant tumors (Figure 2b-d). Interestingly, the combination treatment showed stronger inhibition on primary tumors or distant tumors than ALA-PDT or anti-PD-L1 alone. However, although ALA-PDT alone was highly effective in inhibiting primary tumor growth, it did not show inhibition of distant tumor growth. In comparison, the anti-PD-L1 mAb alone decreased the growth of both primary tumors and distant tumors, although it was not as effective as the combination treatment. All treatments had no effects on the weight of the mice (Figure 2e). The HE staining of distant tumors indicated that that mouse skin in the combined treatment groups had been restored to a normal skin structure with a clear dermal-epidermal boundary. Ki67 staining of distant tumors showed that the positive staining in the combined treatment groups was mainly located in the basal epidermal layer (normal skin without a tumor), while the positive staining in other groups was mainly located in the tumor (Figure 2f). Taken together, these findings showed that ALA-PDT plus PD-L1 blockade inhibits the growth of cSCC *in vivo*.
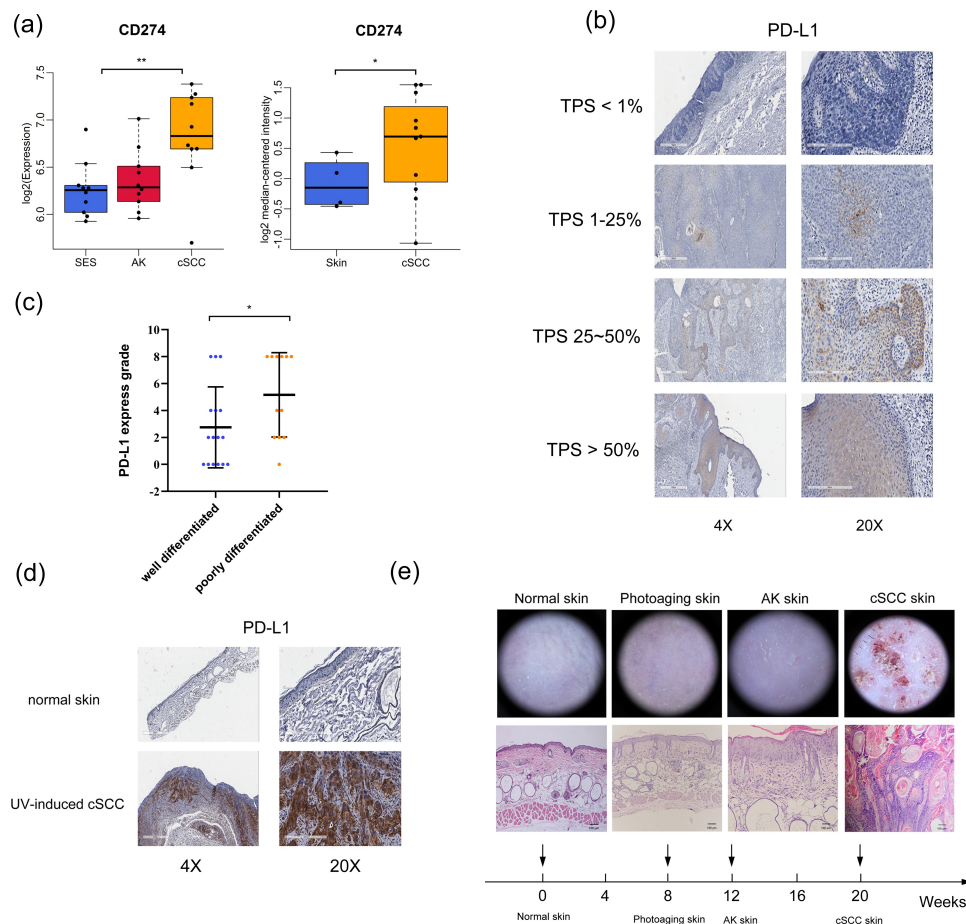
Figure 1. PD-L1 expression is correlated with the progression of cSCC. (a) PD-L1 expression as indicated in the GEO and Oncomine databases. **(b)** PD-L1 expression in cSCC patient tumor tissues, determined by IHC. The tumor proportion score (TPS) represents the proportion of PD-L1-positive expression. **(c)** PD-L1 expression grade of different differentiated cSCC tissues (n = 28). **(d)** PD-L1 expression in UV-induced cSCC mouse tissues as determined by IHC. **(e)** Histological and dermoscopic images of normal skin and cSCC skin during UV-induced cSCC mouse model construction. *$p < 0.05$, **$p < 0.01$; the scale bar is 600 μm for the 4X images, 200 μm for the 20X images and 100 μm for HE staining.

Combined anti-PD-L1 mAb and ALA-PDT therapies are associated with an increased number of tumor-infiltrating lymphocytes

We next observed that the tumors in the combined treatment groups showed an enhanced immunogenic profile pattern when total RNA was isolated from the tumors 24 h after different treatments and analyzed using qPCR. This profile included enhanced expression of TNF-α, IL-12, and IFN-γ and suppressed expression of the immunosuppressive cytokines IL-10, IL-4 and IL-13 in primary tumors and distant tumors (Figure 3a).

Of importance, ALA-PDT alone group exhibited weaker regulatory effects on TNF-α, IL12, IL-4 and IL-13 than the combined treatment groups in primary tumors. And ALA-PDT alone group could not elevate the expression of TNF-α, IFN-γ and decrease the expression of IL-10, IL-4 and IL-13 in distant tumors (Figure 3a-b). These results demonstrated that a combination treatment with an anti-PD-L1 mAb and ALA-PDT inhibited tumor growth by decreasing the expression of some tumor-promoting (immune suppressor) cytokines and increasing tumor suppressor (immune activating) cytokines in the tumor microenvironment.

To test whether the aforementioned *in vivo* antitumor responses observed with combinatorial ALA-PDT and anti-PD-L1 mAb show antitumor immunogenic responses. We dissociated cells from the total tumor mass in each treatment group and assessed the frequency of immune cell subsets, including tumor-infiltrating lymphocytes, by performing flow cytometric analysis. As indicated in Figure 3c-d, primary and distant tumors were harvested from the implanted cSCC mouse model. In the combination-treated mice, the level of CD8$^+$ T cells was significantly increased, and the level of CD4$^+$ T cells exhibited a decreased trend in primary tumors. Moreover, compared to either the ALA-PDT-only or anti-PD-L1 mAb-only treatment, the combination of ALA-PDT and an anti-PD-L1 mAb significantly led to a greater number of CD8$^+$ T cells in primary tumors. However, ALA-PDT alone group had no influence on CD8$^+$ and CD4$^+$ T cells in the distant tumors, while the combination-treated group still increased CD8$^+$ T cells in the distant tumors. This finding suggested that ALA-PDT together with an anti-PD-L1 mAb shows synergistic effects that increase immune infiltration into tumors.
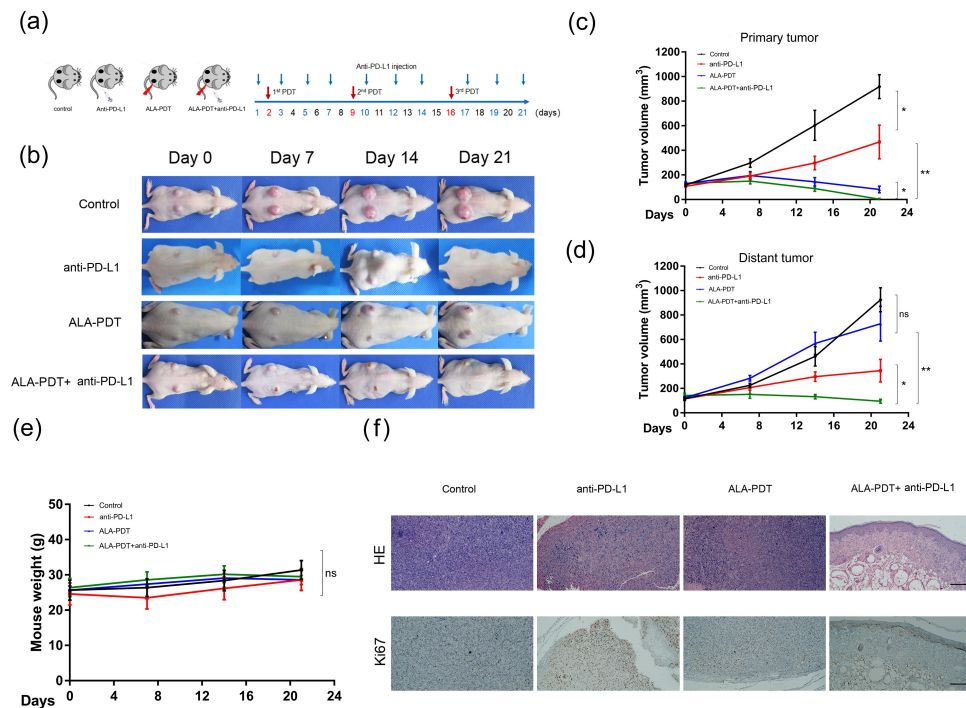
Figure 2. **Synergistic antitumor effects of an anti-PD-L1 mAb and ALA-PDT in an implanted cSCC mouse model. (a)** Diagram of the experimental design of ALA-PDT and an anti-PD-L1 mAb applied to the cSCC mouse model. **(b)** Representative tumor growth in each group. **(c)** Primary tumor growth curve of each group (n = 5 for each group); **(d)** distant tumor growth curve of each group (n = 5 for each group). **(e)** Mouse weight curve of each group. **(f)** Representative HE and Ki67 staining of distant tumors in each group. *$p < 0.05$, **$p < 0.01$; the scale bar is 200 μm.

ALA-PDT plus anti-PD-L1 mAb inhibited tumor growth in a UV-induced cSCC mouse model and stimulated the immunological memory response

We then studied the synergistic antitumor effects of anti-PD-L1 mAb and ALA-PDT in a UV-induced mouse model. The lesions of the UV-induced mouse model were carpet-like and varied in size. Mice were received the treatment shown in Figure 4a. We selected the largest tumor on the backs of the three mice for ALA-PDT (red circle), and an anti-PD-L1 mAb was intraperitoneally injected. As shown in Figure 4a, combination treatment with the anti-PD-L1 mAb and ALA-PDT inhibited overall tumor growth on the backs of the mice, and the tumors were cleared by day 30. Importantly, combination therapy significantly inhibited the number of tumors and reduced the largest tumor volume in three mice (Figure 4b-c). Optical coherence tomography (OCT) analyses and dermoscopic images showed that the epidermis of the mice had been restored and showed a normal skin structure with a clear dermo-epidermal junction (DEJ) on Day 30; however, on Day 14, the epidermis of the mice had been notably thickened, and the DEJ had been wave-shaped and irregular (Figure 4d).

To further investigated the immunological memory effects of ALA-PDT combined with anti-PD-L1 mAb, we rechallenged mice with secondary tumors. Secondary tumor cells were injected 30 days after first tumors elimination by either surgery or combined treatment with anti-PD-L1 mAb and ALA-PDT. We found that ALA-PDT combined with anti-PD-L1 mAb led to obvious inhibition of tumor growth compared

to that in the control group, reflecting the establishment of immune memory against tumor recurrence (Figure 4h). The secretion of cytokines in serum showed that the secretion of TNF-α and IFN-γ was significantly elevated in the combined treatment groups. Overall, the results demonstrated that ALA-PDT plus anti-PD-L1 mAb inhibited tumor growth in a UV-induced cSCC mouse model and stimulated the immunological memory response.

The combined treatment with an anti-PD-L1 mAb and ALA-PDT induced immunogenic cell death

Recently, it has been reported that PDT induces different cancer cell death modalities, such as apoptosis, necrosis, necroptosis, ferroptosis and paraptosis.[30] We further examined cell death modalities induced by the combination treatment of ALA-PDT and anti-PD-L1 mAb. As shown by the immunofluorescence and Western blot results presented in Figure 4 e and f, the Cleaved-caspase 3 and Cleaved-PARP levels were significantly increased in tumor tissues after 24 h of treatment. The data suggested that the combination therapy induced tumor cell apoptosis. Interestingly, the Western blot results shown in Figure 4f indicated that the combination therapy obviously decreased the protein expression levels of SLC7A11 and GPX4 and increased the protein expression level of COX2. The data implied that the combination therapy induced tumor cell ferroptosis. Collectively, these results showed that the combination therapy triggers different regulated cell death modalities, including apoptosis and ferroptosis or their combination.
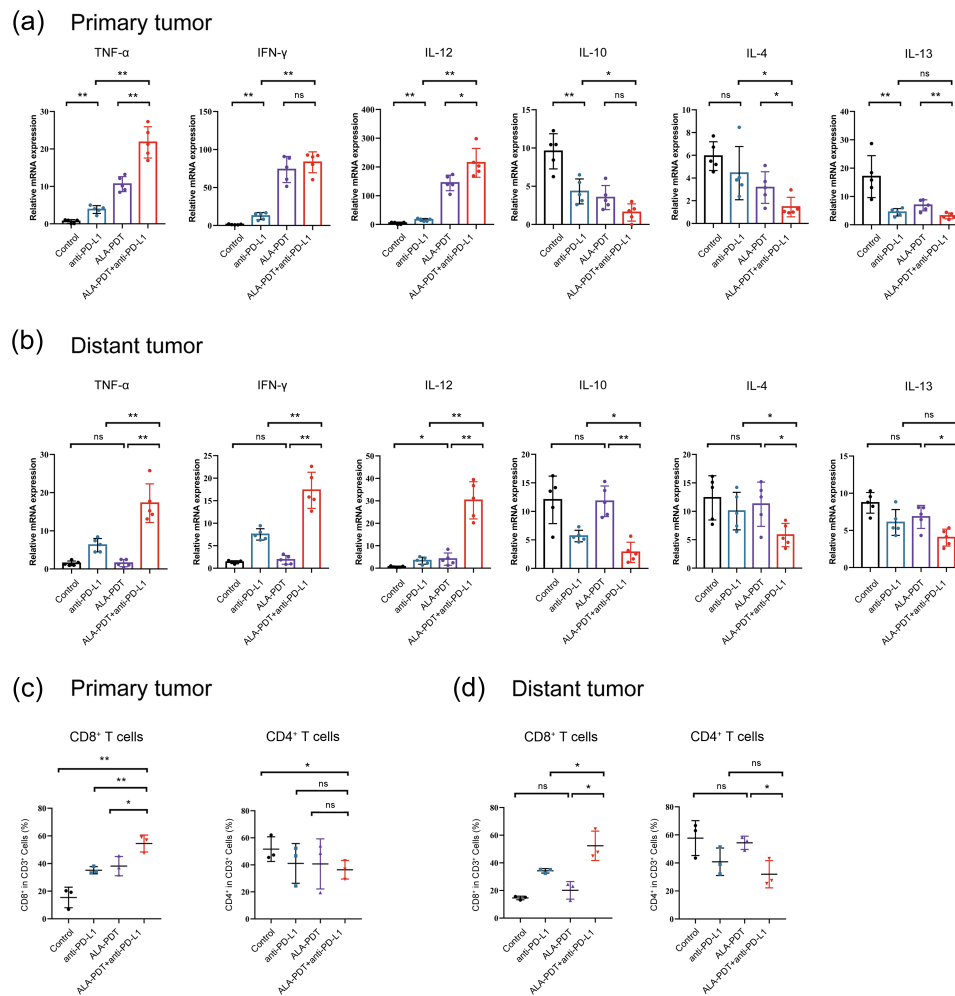
Figure 3. Combined anti-PD-L1 mAb and ALA-PDT therapies are associated with an increased number of tumor-infiltrating lymphocytes. (a-b) Relative mRNA expression was detected by qPCR (n = 5 for each group). **(c-d)** Tumors were collected from each treatment group, and single-cell suspensions were prepared and then stained for specific antibodies against immune cell surface markers (n = 3 for each group). The average percentage of positive surface markers for each group was calculated using flow cytometry. *p < 0.05, **p < 0.01.

We have reported that ALA-PDT can induce ICD in tumor cells, which can elicit a specific antitumor immune response.[14] ICD is an umbrella term for several cell death modalities, including apoptosis and ferroptosis. ICD depends on molecular signals called danger-associated molecular patterns (DAMPs) to activate the innate immune response. DAMPs, including HSPs, CRT, ERp57 and HMGB1, which are released from dying and damaged cells, are molecules derived from host cells, and they signal cell injury or death.[31,32] Western blot analysis of the A431 cell membrane proteins showed that HSP70, ERp57, and CRT levels were obviously elevated in the ALA-PDT alone group and combination group (Figure 4g). The combination group exhibited more greater increases in HSP70, ERp57, and CRT than the ALA-PDT-only group. It has been proven that the upregulated expression of HSPs, ERp57, and CRT is associated with the expression and secretion of DAMPs, which leads to the generation of antitumor immunity. These data indicated that combination therapy induces the acquisition of immunogenic phenotypes in cSCC.

The combined treatment with an anti-PD-L1 mAb and ALA-PDT suppresses tumor growth by altering the TLS-mediated tumor microenvironment

To further investigate how tumor-infiltrating lymphocytes were recruited, we tested the changes in TLSs in cSCCs after ALA-PDT. TLSs represent privileged sites for local DC presentation of neighboring tumor antigens to T cells and activation, proliferation and differentiation of T and B cells.[33,34]

As shown in Figure 5a, tumor tissues from cSCC patients were subjected to immunohistochemistry staining. The tumor tissues (48 h after ALA-PDT) randomly selected from 2 sites showed a significant upregulation in the density of TLSs (yellow circle). Importantly, the structures of the TLSs after ALA-PDT were more complex, showing a follicular-like structure composed of a large number of B cells surrounded by T cells. In addition, the tumor tissues (24 h after ALA-PDT) exhibited newly formed TLS structures and increased T cells and B cells but no follicular-like structures (Figure 5b). We found that
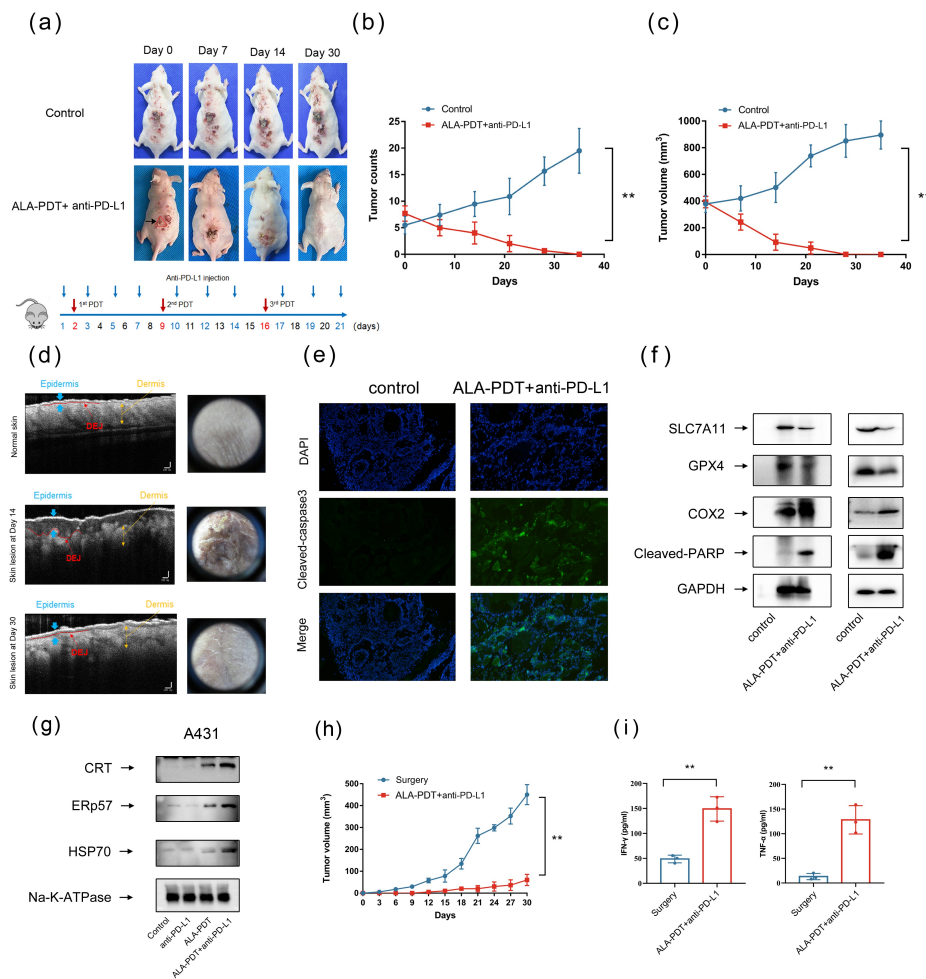
Figure 4. Synergistic antitumor effects of an anti-PD-L1 mAb and ALA-PDT in a UV-induced cSCC mouse model. (a) Representative tumor growth of the UV-induced cSCC mouse model. ALA-PDT was applied to tumors in the red circle, and anti-PD-L1 mAb was intraperitoneally injected. **(b)** Tumor count curve of the UV-induced cSCC mouse model (n = 3 for each group). **(c)** Largest tumor growth curve of the UV-induced cSCC mouse model (n = 3 for each group). **(d)** OCT analyses of mouse skin structure, left panel. Dermoscopic images of mouse skin, right panel. **(e)** After 24 h of treatment, immunofluorescence of tumor tissue in the UV-induced cSCC mouse model was detected. **(f)** After 24 h of treatment, tumor tissue lysates of the UV-induced cSCC mouse model (left panel) and implanted cSCC mouse model (right panel) were subjected to Western blotting with the indicated antibodies. The blots were probed with GAPDH as the loading control. **(g)** After 6 h of treatment, A431 cell membrane lysates were subjected to Western blotting using the indicated antibodies. The blots were probed with Na-K-ATPase as the loading control. **(h)** Tumor growth curves of rechallenged tumors inoculated 30 days post-elimination of their first tumors by either surgery or combined treatment with anti-PD-L1 mAb and ALA-PDT (n = 3 for each group). **(i)** Cytokine levels of IFN-γ and TNF-α in sera from mice isolated 7 days after mice were rechallenged with secondary tumors. *$p < 0.05$, **$p < 0.01$.

the density of TLSs was increased in 2 of the 5 cSCC patient tissues collected 24 hours after PDT and in 3 of the 5 cSCC patient tissues collected 48 hours after PDT (data not shown). We verified the presence of TLS formation-related chemokines in mouse tumor tissues and found that combination therapy promoted an increase in TLS formation-related chemokines[20,35] such as CCL2, CCL8, CCL19, CCL21a, CCL21b, CXCL9 and CXCL13 (Figure 6a). In addition, the tumor tissues (24 h after ALA-PDT and anti-PD-L1) exhibited newly formed TLS structures and increased T cells and B cells in mouse tumor tissues (Figure 6b and c). Taken together, our data support the notion that the combination of an anti-PD-L1 mAb and ALA-PDT modulates antitumor immunity by altering the TLS-mediated tumor microenvironment.

Discussion

Tumor immunotherapy has attracted widespread attention as a promising treatment. Checkpoint blockades, such as anti-PD-1, anti-PD-L1, and anti-CTLA-4, provide effective therapeutic methods for tumor patients. However, the objective response rate remains low in cSCC (not enough 50% objective response). Thus, novel therapeutic approaches are needed to improve the response rate and to increase the therapeutic effect.

ALA-PDT is dominantly used to treat actinic keratoses, squamous cell carcinoma in situ, superficial and certain thin basal cell carcinomas. The curative effect of ALA-PDT in cSCC, however, remains under debate. Some scholars believe that it shows poor efficacy in treating invasive cSCC.[10,12] Others believe that the PDT-induced immune response is too weak to inhibit the growth of the remaining tumor cells.[36] Therefore, in view of the many advantages of ALA-PDT, such as its

(a)

(b)
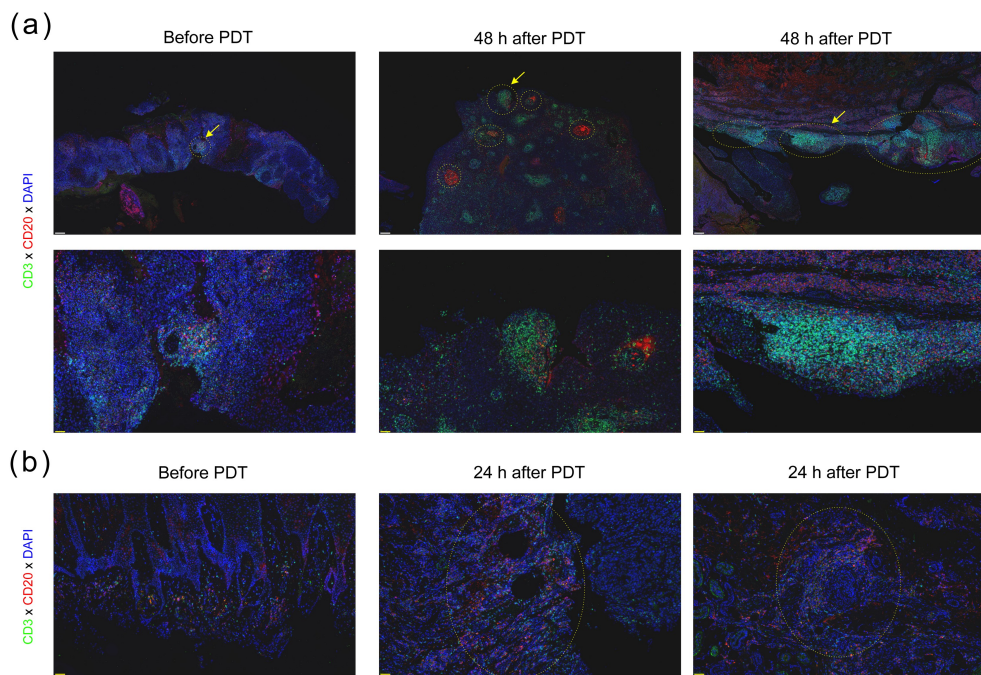
Figure 5. ALA-PDT suppresses tumor growth by altering the TLS-mediated tumor microenvironment in cSCC patients. (a) Tumor tissues from cSCC patients were subjected to immunohistochemistry staining. Tumor tissues (48 h after ALA-PDT) were randomly selected from 2 sites. The yellow circles show TLSs, the yellow arrows indicate the enlarged area in the image below. (b) Tumor tissues (24 h after ALA-PDT) were randomly selected from 2 sites. The yellow circles show TLSs. The scale bar is 200 μm (white) and 50 μm (yellow).

noninvasive nature, favorable safety and antitumor immunity, improving the effects of PDT through combination therapy is a promising tumor treatment strategy.

ALA-PDT destroys tumors and stimulates immune responses by promoting tumor antigen presentation, thus increasing the response rates to checkpoint blockade antibodies.[37,38] Some studies have aimed to combine nanoparticle-based PDT with checkpoint blockade therapy as a promising strategy for potentiating antitumor therapeutic efficacy.[39] For example, Yuan et al. reported that through the use of multifunctional nanoparticles, PDT synergizes with a PD-L1 checkpoint blockade for immunotherapy of colorectal cancer.[40] Liu et al. presented a tumor microenvironment-responsive biodegradable CaCO3/MnO2-based nanoplatform for enhanced photodynamic therapy and improved PD-L1 immunotherapy in lung cancer.[41] However, few studies have reported the combined effect of ALA-PDT and an anti-PD-L1 mAb in cSCC. Considering that photosensitizer ALA-based PDT has been used in clinical treatment, we believe that the combination of ALA-PDT and an anti-PD-L1 mAb in cSCC is worthy of further study.

In this study, we showed that the PD-L1 blockade potentiates the antitumor effects of ALA-PDT and optimizes the tumor microenvironment in cSCC. ALA-PDT combined with an anti-PD-L1 mAb killed tumor cells by apoptosis and/or ferroptosis mediated immunogenic cell death (ICD) and subsequently stimulated the immune response. Some studies have also demonstrated that different types of photosensitizers-induced PDT could trigger ICD. For example, Victoria et al. reported that PDT based on photosens and photodithazine

could induce ICD in glioma and fibrosarcoma.[19] Lang et al. found that radiotherapy and immunotherapy promote ferroptosis via synergistic repression of SLC7A1.[42] These results suggested that ROS-based treatment such as PDT could modulate the immune system through ICD. Furthermore, we found that ALA-PDT recruited TLS-like intratumoral lymphoid aggregates. Combination therapy increased the expression of chemokines associated with TLS formation. Our recent study has shown that ALA-PDT-treated apoptotic cells are sources of tumor antigens that stimulate the maturation of DCs.[14,43] T cell immunity is initiated by mature DCs, preventing tumor growth. Considering our results, we found that combination therapy evoked an antitumor immune response and that this response was likely a result of four mechanisms. First, the combination therapy induced ICD and thus elicited an immune response. Second, the combination therapy induced DC maturation and migration to lymph nodes. Third, the combination therapy recruited TLS-like intratumoral lymphoid aggregates, promoted T cell infiltration and increased the proportion of CD8 + T cells. Fourth, due to the PD-L1 inhibition of tumors, the combination therapy significantly promoted the generation of tumor-specific effector T cells and enhanced their infiltration in both primary and distant tumors, resulting in not only tumor eradication at primary sites but also a systemic antitumor immune response that eliminated distant tumors.

TLSs reflect lymphoid neogenesis in peripheral tissues upon long-lasting exposure to inflammatory signaling mediated by chemokines and cytokines. TLSs are associated with favorable prognosis in most solid malignancies studied thus far,
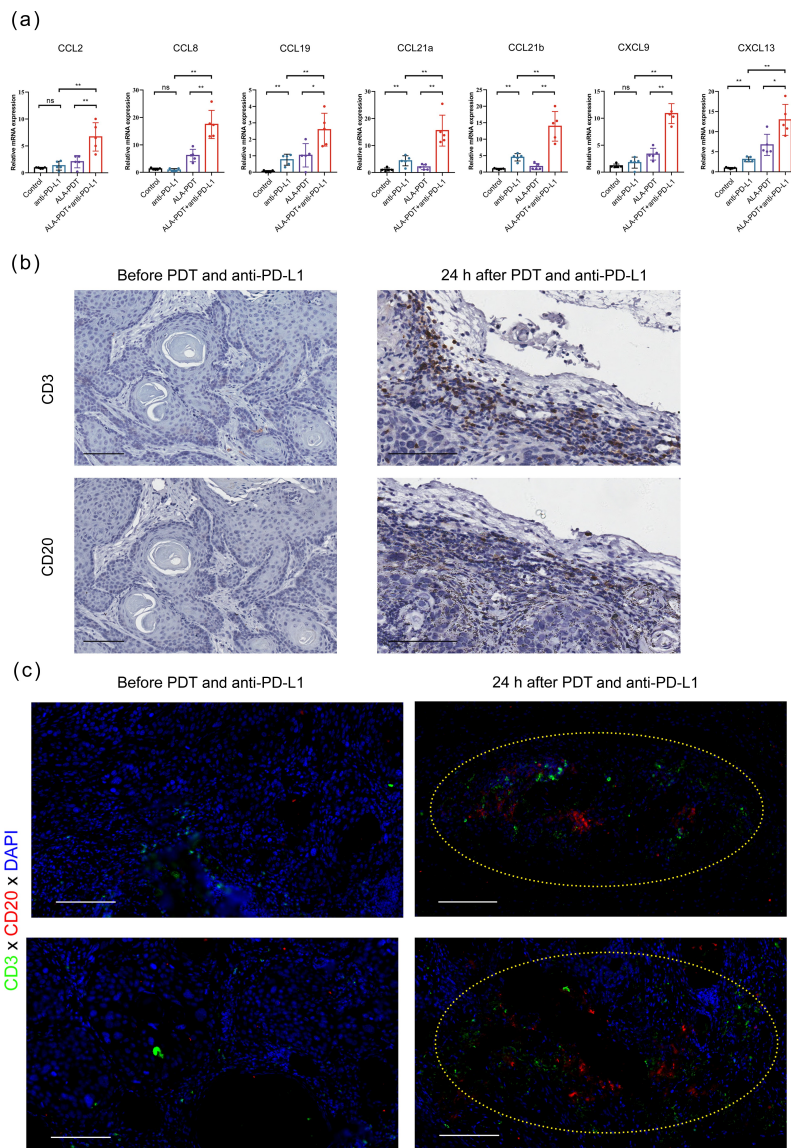
Figure 6. The combined treatment with an anti-PD-L1 mAb and ALA-PDT suppresses tumor growth by altering the TLS-mediated tumor microenvironment in UV-induced cSCC mouse model. (a) After 24 h of treatment, tumor tissues of the UV-induced cSCC mouse model were collected, and relative mRNA expression was detected by qPCR. **(b)** Tumor tissues (before or 24 h after ALA-PDT and anti-PD-L1) from UV-induce cSCC mouse were subjected to immunohistochemistry staining of consecutive sections. **(c)** Tumor tissues of mice (before or 24 h after ALA-PDT and anti-PD-L1) were subjected to immunohistochemistry staining and randomly selected from 2 sites. The yellow circles show TLSs. $*p < 0.05$, $**p < 0.01$; the scale bar is 100 µm.

illustrating their capacity to induce a systemic long-lasting antitumor response. Several approaches are being developed using chemokines, cytokines, antibodies, antigen-presenting cells or synthetic scaffolds to induce TLS formation. Strategies, such as the use of ALA-PDT, to induce TLS neogenesis in tumors and, in this case, in combination with immune checkpoint inhibitors, represent promising avenues to cancer treatment.

In conclusion, the combination of ALA-PDT and an anti-PD-L1 checkpoint blockade effectively inhibited the growth of both local tumors and distant tumors. The combination of ALA-PDT and anti-PD-L1 stimulated the TLS-mediated antitumor immune response and the immunological memory response during cancer treatment. Therefore, this strategy may provide potential effective clinical benefits by expanding the percentage of cSCC patients who respond to anti-PD-L1 immune checkpoint therapy.

Author contributions

Qingyu Zeng, Guolong Zhang and Xiuli Wang conceived the project and designed the experiments. Guorong Yan performed the bioinformatics analyses. Jiayi Yang, Jie Ji, Yuhao Wu, Qi Chen and Jia Liu performed the animal experiments. Peiru Wang and Linglin Zhang supervised the overall execution of the experiments. The manuscript was written by Qingyu Zeng. All authors have read and approved the final manuscript.

Disclosure statement

Funding

ORCID

Qingyu Zeng 🆔 http://orcid.org/0000-0003-3170-7706
Jiayi Yang 🆔 http://orcid.org/0000-0002-1604-7503
Guorong Yan 🆔 http://orcid.org/0000-0001-9200-2959
Guolong Zhang 🆔 http://orcid.org/0000-0002-9207-1361
Xiuli Wang 🆔 http://orcid.org/0000-0002-0722-1274

Data availability

References

1. Schmults CD, Karia PS, Carter JB, Han J, Qureshi AA. Factors predictive of recurrence and death from cutaneous squamous cell carcinoma: a 10-year, single-institution cohort study. JAMA Dermatol. 2013;149(5):541–547. doi:10.1001/jamadermatol.2013.2139.

2. Brantsch KD, Meisner C, Schonfisch B, Trilling B, Wehner-Caroli J, Rocken M, Breuninger H. Analysis of risk factors determining prognosis of cutaneous squamous-cell carcinoma: a prospective study. Lancet Oncol. 2008;9(8):713–720. doi:10.1016/S1470-2045(08)70178-5.

3. Page DB, Postow MA, Callahan MK, Allison JP, Wolchok JD. Immune modulation in cancer with antibodies. Annu Rev Med. 2014;65(1):185–202. doi:10.1146/annurev-med-092012-112807.

4. Ribas A. Releasing the Brakes on Cancer Immunotherapy. N Engl J Med. 2015;373(16):1490–1492. doi:10.1056/NEJMp1510079.

5. Grob JJ, Gonzalez R, Basset-Seguin N, Vornicova O, Schachter J, Joshi A, Meyer N, Grange F, Piulats JM, Bauman JR, et al. Pembrolizumab Monotherapy for Recurrent or Metastatic Cutaneous Squamous Cell Carcinoma: a Single-Arm Phase II Trial (KEYNOTE-629. J Clin Oncol. 2020;38(25):2916–2925. doi:10.1200/JCO.19.03054.

6. Kubli SP, Berger T, Araujo DV, Siu LL, Mak TW. Beyond immune checkpoint blockade: emerging immunological strategies. Nat Rev Drug Discov. 2021 Dec;20(12):899–919. doi:10.1038/s41573-021-00155-y. PMID: 33686237.

7. Skaria AM. European guidelines for topical PDT part 1 JEADV. J Eur Acad Dermatol Venereol. 2013;28(5):673. doi:10.1111/jdv.12258.

8. Cohen DK, Lee PK. Photodynamic therapy for non-melanoma skin cancers. Cancers (Basel). 2016;8(10):90. doi:10.3390/cancers8100090.

9. Zhang GL, Keyal U, Shi L, Wang PR, Zhang LL, Bhatta AK, Wu YH, Fang S, Wang XL. Photodynamic therapy as an alternative treatment in patients with invasive cutaneous SCC where surgery is not feasible: single center experience. Photodiagnosis Photodyn Ther. 2020;32:101980. doi:10.1016/j.pdpdt.2020.101980.

10. Keyal U, Bhatta AK, Zhang G, Wang XL. Present and future perspectives of photodynamic therapy for cutaneous squamous cell carcinoma. J Am Acad Dermatol. 2019;80(3):765–773. doi:10.1016/j.jaad.2018.10.042.

11. Wang P, Zhang L, Zhang G, Zhou Z, Zhang H, Zhao Z, Shi L, Wang X. Successful treatment of giant invasive cutaneous squamous cell carcinoma by plum-blossom needle assisted photodynamic therapy sequential with imiquimod: case experience. Photodiagnosis Photodyn Ther. 2018;21:393–395. doi:10.1016/j.pdpdt.2017.12.010.

12. Gilaberte Y, Milla L, Salazar N, Vera-Alvarez J, Kourani O, Damian A, Rivarola V, Roca MJ, Espada J, Gonzalez S, et al. Cellular intrinsic factors involved in the resistance of squamous cell carcinoma to photodynamic therapy. J Invest Dermatol. 2014;134(9):2428–2437. doi:10.1038/jid.2014.178.

13. Lansbury L, Bath-Hextall F, Perkins W, Stanton W, Leonardi-Bee J. Interventions for non-metastatic squamous cell carcinoma of the skin: systematic review and pooled analysis of observational studies. BMJ. 2013;347:f6153. doi:10.1136/bmj.f6153.

14. Ji J, Zhang Y, Chen WR, Wang X. DC vaccine generated by ALA-PDT-induced immunogenic apoptotic cells for skin squamous cell carcinoma. Oncoimmunology. 2016;5(6):e1072674. doi:10.1080/2162402X.2015.1072674.

15. Zhao Z, Zhang H, Zeng Q, Wang P, Zhang G, Ji J, Li M, Shen S, Wang X. Exosomes from 5-aminolevulinic acid photodynamic therapy-treated squamous carcinoma cells promote dendritic cell maturation. Photodiagnosis Photodyn Ther. 2020;30:101746. doi:10.1016/j.pdpdt.2020.101746.

16. Gomes-da-silva LC, Zhao L, Arnaut LG, Kroemer G, Kepp O. Redaporfin induces immunogenic cell death by selective destruction of the endoplasmic reticulum and the Golgi apparatus. Oncotarget. 2018;9(58):31169–31170. doi:10.18632/oncotarget.25798.

17. Gomes-da-silva LC, Zhao L, Bezu L, Zhou H, Sauvat A, Liu P, Durand S, Leduc M, Souquere S, Loos F, et al. Photodynamic therapy with redaporfin targets the endoplasmic reticulum and Golgi apparatus. EMBO J. 2018;37. doi:10.15252/embj.201798354.

18. Panzarini E, Inguscio V, Fimia GM, Dini L. Rose Bengal acetate photodynamic therapy (RBAc-PDT) induces exposure and release of damage-associated molecular patterns (DAMPs) in human HeLa cells. PLoS One. 2014;9:e105778. doi:10.1371/journal.pone.0105778.

19. Turubanova VD, Balalaeva IV, Mishchenko TA, Catanzaro E, Alzeibak R, Peskova NN, Efimova I, Bachert C, Mitroshina EV, Krysko O, et al. Immunogenic cell death induced by a new photodynamic therapy based on photosens and photodithazine. J Immunother Cancer. 2019;7(1):350. doi:10.1186/s40425-019-0826-3.

20. Sautes-Fridman C, Petitprez F, Calderaro J, Fridman WH. Tertiary lymphoid structures in the era of cancer immunotherapy. Nat Rev Cancer. 2019;19(6):307–325. doi:10.1038/s41568-019-0144-6.

21. Dieu-Nosjean MC, Giraldo NA, Kaplon H, Germain C, Fridman WH, Sautes-Fridman C. Tertiary lymphoid structures, drivers of the anti-tumor responses in human cancers. Immunol Rev. 2016;271:260–275. doi:10.1111/imr.12405.

22. Helmink BA, Reddy SM, Gao J, Zhang S, Basar R, Thakur R, Yizhak K, Sade-Feldman M, Blando J, Han G, et al. B cells and tertiary lymphoid structures promote immunotherapy response. Nature. 2020;577:549–555.

23. Cabrita R, Lauss M, Sanna A, Donia M, Skaarup Larsen M, Mitra S, Johansson I, Phung B, Harbst K, Vallon-Christersson J, et al. Tertiary lymphoid structures improve immunotherapy and survival in melanoma. Nature. 2020;577:561–565.

24. Petitprez F, de Reynies A, Keung EZ, Chen TW, Sun CM, Calderaro J, Jeng YM, Hsiao LP, Lacroix L, Bougouin A, et al. B cells are associated with survival and immunotherapy response in sarcoma. Nature. 2020;577:556–560. doi:10.1038/s41586-019-1906-8.

25. Wang X, Shi L, Tu Q, Wang H, Zhang H, Wang P, Zhang L, Huang Z, Zhao F, Luan H, et al. Treating cutaneous squamous cell carcinoma using 5-aminolevulinic acid polylactic-co-glycolic acid nanoparticle-mediated photodynamic therapy in a mouse model. Int J Nanomedicine. 2015;10:347–355. doi:10.2147/IJN.S71245.

26. Zhang G, Yan G, Fu Z, Wu Y, Wu F, Zheng Z, Fang S, Gao Y, Bao X, Liu Y, et al. Loss of retinoic acid receptor-related receptor alpha (Roralpha) promotes the progression of UV-induced cSCC. Cell Death Dis. 2021;12:247. doi:10.1038/s41419-021-03525-x.

27. Zeng Q, Zhang H, Qin J, Xu Z, Gui L, Liu B, Liu C, Xu C, Liu W, Zhang S, et al. Rapamycin inhibits BAFF-stimulated cell proliferation and survival by suppressing mTOR-mediated PP2A-Erk1/2 signaling pathway in normal and neoplastic B-lymphoid cells. Cell Mol Life Sci. 2015;72:4867–4884. doi:10.1007/s00018-015-1976-1.

28. Que SKT, Zwald FO, Schmults CD. Cutaneous squamous cell carcinoma: incidence, risk factors, diagnosis, and staging. J Am Acad Dermatol. 2018;78:237–247. doi:10.1016/j.jaad.2017.08.059.

29. Garcovich S, Colloca G, Sollena P, Andrea B, Balducci L, Cho WC, Bernabei R, Peris K. Skin cancer epidemics in the elderly as an emerging issue in geriatric oncology. Aging Dis. 2017;8:643–661. doi:10.14336/AD.2017.0503.

30. Mishchenko TA, Balalaeva IV, Vedunova MV, Krysko DV. Ferroptosis and photodynamic therapy synergism: enhancing anticancer treatment. Trends Cancer. 2021;7:484–487. doi:10.1016/j.trecan.2021.01.013.

31. Aaes TL, Verschuere H, Kaczmarek A, Heyndrickx L, Wiernicki B, Delrue I, De Craene B, Taminau J, Delvaeye T, Bertrand MJM, et al. Immunodominant AH1 antigen-deficient necroptotic, but not apoptotic, murine cancer cells induce antitumor protection. J Immunol. 2020;204:775–787. doi:10.4049/jimmunol.1900072.

32. Galluzzi L, Vitale I, Warren S, Adjemian S, Agostinis P, Martinez AB, Chan TA, Coukos G, Demaria S, Deutsch E, et al. Consensus guidelines for the definition, detection and interpretation of immunogenic cell death. J Immunother Cancer. 2020;8: e000337. doi:10.1136/jitc-2019-000337.

33. Martinet L, Garrido I, Filleron T, Le Guellec S, Bellard E, Fournie JJ, Rochaix P, Girard JP. Human solid tumors contain high endothelial venules: association with T- and B-lymphocyte infiltration and favorable prognosis in breast cancer. Cancer Res. 2011;71:5678–5687. doi:10.1158/0008-5472.CAN-11-0431.

34. Germain C, Gnjatic S, Tamzalit F, Knockaert S, Remark R, Goc J, Lepelley A, Becht E, Katsahian S, Bizouard G, et al. Presence of B cells in tertiary lymphoid structures is associated with a protective immunity in patients with lung cancer. Am J Respir Crit Care Med. 2014;189:832–844. doi:10.1164/rccm.201309-1611OC.

35. Messina JL, Fenstermacher DA, Eschrich S, Qu X, Berglund AE, Lloyd MC, Schell MJ, Sondak VK, Weber JS, Mule JJ. 12-Chemokine gene signature identifies lymph node-like structures in melanoma: potential for patient selection for immunotherapy? Sci Rep. 2012;2:765. doi:10.1038/srep00765.

36. Yang Y, Hu Y, Wang H. Targeting antitumor immune response for enhancing the efficacy of photodynamic therapy of cancer: recent advances and future perspectives. Oxid Med Cell Longev. 2016;2016:5274084. doi:10.1155/2016/5274084.

37. Maeding N, Verwanger T, Krammer B. Boosting Tumor-Specific Immunity Using PDT. Cancers (Basel). 2016;8(10):91. doi:10.3390/cancers8100091.

38. Hwang HS, Shin H, Han J, Na K. Combination of photodynamic therapy (PDT) and anti-tumor immunity in cancer therapy. J Pharm Investig. 2018;48(2):143–151. doi:10.1007/s40005-017-0377-x.

39. Kaleta-Richter M, Kawczyk-Krupka A, Aebisher D, Bartusik-Aebisher D, Czuba Z, Cieslar G. The capability and potential of new forms of personalized colon cancer treatment: immunotherapy and photodynamic therapy. Photodiagnosis Photodyn Ther. 2019;25:253–258. doi:10.1016/j.pdpdt.2019.01.004.

40. Yuan Z, Fan G, Wu H, Liu C, Zhan Y, Qiu Y, Shou C, Gao F, Zhang J, Yin P, et al. Photodynamic therapy synergizes with PD-L1 checkpoint blockade for immunotherapy of CRC by multifunctional nanoparticles. Mol Ther. 2021;29(10):2931–2948. doi:10.1016/j.ymthe.2021.05.017.

41. Liu Y, Pan Y, Cao W, Xia F, Liu B, Niu J, Alfranca G, Sun X, Ma L, de la Fuente JM, et al. A tumor microenvironment responsive biodegradable CaCO3/MnO2- based nanoplatform for the enhanced photodynamic therapy and improved PD-L1 immunotherapy. Theranostics. 2019;9:6867–6884. doi:10.7150/thno.37586.

42. Lang X, Green MD, Wang W, Yu J, Choi JE, Jiang L, Liao P, Zhou J, Zhang Q, Dow A, et al. Radiotherapy and immunotherapy promote tumoral lipid oxidation and ferroptosis via synergistic repression of SLC7A11. Cancer Discov. 2019;9(12):1673–1685. doi:10.1158/2159-8290.CD-19-0338.

43. Ji J, Fan Z, Zhou F, Wang X, Shi L, Zhang H, Wang P, Yang D, Zhang L, Chen WR, et al. Improvement of DC vaccine with ALA-PDT induced immunogenic apoptotic cells for skin squamous cell carcinoma. Oncotarget. 2015;6(19):17135–17146. doi:10.18632/oncotarget.3529.